

## Low Gut Microbial Diversity Augments Estrogen-driven Pulmonary Fibrosis in Female-Predominant Interstitial Lung Disease

**Authors:** Ozioma S. Chioma<sup>1</sup>, Elizabeth Mallott<sup>2</sup>, Binal Shah-Gandhi<sup>1</sup>, ZaDarreyal Wiggins<sup>1</sup>, Madison Langford<sup>1</sup>, Andrew William Lancaster<sup>1</sup>, Alexander Gelbard<sup>3</sup>, Hongmei Wu<sup>3</sup>, Joyce E. Johnson<sup>4</sup>, Lisa Lancaster<sup>1</sup>, Erin M. Wilfong<sup>1</sup>, Leslie J. Crofford<sup>1,2</sup>, Courtney G. Montgomery<sup>5</sup>, Luc Van Kaer<sup>4</sup>, Seth Bordenstein<sup>6</sup>, Dawn C. Newcomb<sup>1,4</sup>, Wonder Puryear Drake<sup>1,4\*</sup>

**Affiliations:** Departments of <sup>1</sup>Medicine, Vanderbilt University School of Medicine, Nashville, TN; <sup>2</sup>Department of Biology, Washington University in St. Louis, St. Louis, MO; <sup>3</sup>Otolaryngology-Head and Neck Surgery, <sup>4</sup>Pathology, Microbiology, and Immunology, Vanderbilt University School of Medicine, Nashville, TN; <sup>5</sup>Genes and Human Disease Research Program, Oklahoma Medical Research Foundation, Oklahoma City, OK; <sup>6</sup>Department of Biology and Entomology, Pennsylvania State University, College Station, PA

**\*Corresponding author:** Wonder P. Drake, M.D., 21st Avenue South, Medical Center North, Room A2310, Nashville, TN 37232

Email: wonder.drake@vumc.org; ORCID ID: 0000-0001-9406-3130

**Conflict of interest statement:** L. Van Kaer is a member of the scientific advisory board of Isu Abxis Co., Ltd. (South Korea). The other authors have declared that no conflict of interest exists.

## Abstract

Although profibrotic cytokines such as IL-17A and TGF- $\beta$ 1 have been implicated in interstitial lung disease (ILD) pathogenesis, interactions between gut dysbiosis, gonadotrophic hormones and molecular mediators of profibrotic cytokine expression, such as phosphorylation of STAT3, have not been defined. Here we show by chromatin immunoprecipitation sequencing (ChIP-seq) analysis of primary human CD4+ T cells that regions within the *STAT3* locus are significantly enriched for binding by the transcription factor estrogen receptor alpha (ER $\alpha$ ). Using the murine model of bleomycin-induced pulmonary fibrosis, we found significantly increased regulatory T cells compared to Th17 cells in the female lung. Genetic absence of *ESR1* or ovariectomy in mice significantly increased pSTAT3 and IL-17A expression in pulmonary CD4+ T cells, which was reduced after repletion of female hormones. Remarkably, there was no significant reduction in lung fibrosis under either condition, suggesting that factors outside of ovarian hormones also contribute. Assessment of lung fibrosis among menstruating females in different rearing environments revealed that environments favoring gut dysbiosis augment fibrosis. Furthermore, hormone repletion following ovariectomy further augmented lung fibrosis, suggesting pathologic interactions between gonadal hormones and gut microbiota on lung fibrosis severity. Analysis in female sarcoidosis patients revealed a significant reduction in pSTAT3 and IL-17A levels and a concomitant increase in TGF- $\beta$ 1 levels in CD4+ T cells, compared to male sarcoidosis patients. These studies reveal that estrogen is profibrotic in females and that gut dysbiosis in menstruating females augments lung fibrosis severity, supporting a critical interaction between gonadal hormones and gut flora in lung fibrosis pathogenesis.

**Word Count: 246**

## Introduction

An ever-growing synergy of human and animal investigations support an important role of sex hormone regulation of immunity in the pathophysiology of chronic lung diseases [1, 2]. IL-17 signaling has been implicated in numerous chronic lung diseases, such as idiopathic pulmonary fibrosis (IPF), lung cancer and pulmonary sarcoidosis [1, 3-5]. Moreover, striking clinical disparities according to sex are observed in Th17 cell-mediated diseases. For example, although the incidence of IPF is higher in men, female sex is predictive of better IPF clinical outcomes [6-8]. Among patients with pulmonary arterial hypertension, female patients have better survival than males [9-11]. These observations support the urgent need to identify relevant sex-specific mechanisms in chronic pulmonary inflammation.

Independent reports demonstrate that profibrotic signaling pathways converge on STAT3, an important molecular checkpoint for tissue fibrosis [12, 13]. Immune cells, including CD4+ T cells, produce IL-6 which enhances collagen production through induction of JAK/STAT3/IL-17A or JAK/ERK/TGF- $\beta$ 1 signaling in local and systemic environments [14-17]. Distinctions in clinical outcome by sex support an investigation of an interplay of female gonadotrophic hormones with STAT3-dependent induction of profibrotic cytokine expression. Interactions of the alpha subunit of the estrogen receptor (ER $\alpha$ ) and STAT3 protein, both transcription factors, have been reported in breast cancers of epithelial origin, noting enhanced epithelial-mesenchymal transition (EMT), as well as augmented tumor metastasis [18]. Yet the immunologic consequences of ER $\alpha$  binding to the *STAT3* gene in CD4+ T cells of patients with lung fibrosis remain unexplored.

The observed disparate clinical outcomes in chronic lung diseases by sex support investigation of the impact of gonadotrophic hormones on STAT3 signaling, specifically in the context of the profibrotic cytokines, IL-17A and TGF- $\beta$ 1. Here, we report that human females experiencing loss of lung function due to progressive fibrosis, as well as female murine models of bleomycin-induced lung fibrosis, demonstrate increased T

regulatory cells with TGF- $\beta$ 1 expression (immunosuppressive) in the fibrotic lung microenvironment. Lower estrogen states, such as those found in males and ovariectomized female mice, reveal increased IL-17A expression due to elevated percentages of pulmonary Th17 cells (proinflammatory). Moreover, investigation of this estrogen-adaptive immunity interplay in distinct environments reveals that low gut microbial diversity further increases estrogen-induced lung fibrosis. This data demonstrates a distinct sex-specific role for STAT3 signaling in CD4+ T cells, thus paving the way for developing personalized (e.g. sex-based) immunotherapeutic strategies for chronic lung inflammation.

## 2. Materials and Methods

### *Human Study Approval*

To participate in this study, all human subjects signed a written informed consent form, and patients were enrolled from Vanderbilt University Medical Center. All human studies were approved by the appropriate institutional review board (VUMC 040187).

### *Study Population.*

For inclusion in this study, the clinical and radiographic criteria used to define sarcoidosis were applied [19]. IPF subjects were defined according to recent American Thoracic Society (ATS) guidelines [20] and systemic sclerosis patients were defined according to the 2013 American College of Rheumatology criteria [21]. Clinical lung progression was defined as previously described [22]. Pulmonary function testing was performed as clinically indicated. FVC decline was defined as a relative reduction of  $\geq 10\%$  in percent predicted FVC. There were four human cohorts in this study: 25 healthy controls (7 males, 18 females), 31 sarcoidosis patients (11 males, 20 females), idiopathic pulmonary fibrosis (IPF) patients (36 males, 9 females), and scleroderma patients (5 males, 6 females). Information on study subject demographics is provided in **Table 1**.

### *Peripheral Blood Mononuclear Cells Isolation and Storage.*

Ficoll-Hypaque density gradient centrifugation method was used to isolate peripheral blood mononuclear cells (PBMCs) from whole blood of all four human cohorts in this study; healthy controls, sarcoidosis, IPF and scleroderma patients as previously described [23, 24]. PBMCs were then stored in fetal bovine serum containing 10% dimethyl sulfoxide (DMSO) at a concentration of  $10 \times 10^6$  cells/mL, in a -80°C freezer before being transferred to liquid nitrogen for prolonged storage, or before use.

### *Chromatin Immunoprecipitation Sequencing (ChIP-Seq) Library preparation.*

Primary CD4+ T cells were negatively selected using immunomagnetic bead separation (STEMCELL, EasySep #17951). Approximately one to 2.5 million total T cells were obtained from five to 10 million PBMCs. T cells were first incubated with 2mM disuccinimidyl glutarate for 35 minutes at room temperature, then formaldehyde was added to a final concentration of 1% and cells were incubated for another 10 minutes at room temperature [25]. Nuclei were isolated using the Covaris truChIP Chromatin Shearing Kit and fragmented by sonication. Immunoprecipitation was performed using an anti-ER $\alpha$  antibody (Cell Signaling #8644) and protein A+G magnetic beads. Chromatin were de-crosslinked and purified by AMPure XP beads. ChIP-seq libraries were prepared according to Illumina protocols and were sequenced using 75bp paired-end sequencing on an Illumina NextSeq, producing an average of 135,924,844 reads per library.

### *Sequencing alignment and peak calling.*

ChIP-seq reads were examined for technical artifacts with FastQC. No aberrant technical behavior was identified. Reads were trimmed for adapter sequences and decontaminated for sequencing artifacts by bbdruk. Trimming options were set to ktrim=right trimming, mink=11, hdist=1, qin=33, tpe and tbo options enabled. BBduk's list of illumina sequencing adapters was used to perform adapter trimming. Decontamination was done against phiX adapters and bbdruk's database of sequencing

artifacts. Decontaminated reads were aligned to version GRCh38 of the human reference genome using BWA-mem [26] with the following options: -L 100 -k 8 -O 5. Following alignment, peaks were called with respect to the input chromatin library using MACS2 [27], with the following options: --nomodel –shift -100 –extsize 200 -g hs -q 0.05 -f BAMPE –keep-dup all –broad.

#### *Murine Model of Pulmonary Fibrosis.*

All murine procedures were performed according to the protocol approved by the Institutional Animal Care and Use Committee at Vanderbilt University Medical Center (protocol #M1700043). For the murine model of bleomycin-induced pulmonary fibrosis, 5- to 8-week-old mice weighing approximately 17-22 g were used. Mice were anesthetized by intraperitoneal injection of 80 µl of 20mg/ml Ketamine/1.8 mg/ml Xylazine solution. Then 75 µl containing 0.04 Units of bleomycin (Novaplus Lake Forest IL) in saline or equal volume of saline (0.9% sodium chloride) (Hospira Inc, Lake forest IL) as control were administrated intranasally to wild-type or ESR-1/- mice as previously described [28]. Lungs were harvested for histology, flow cytometry, or single-cell isolation as previously described [16]. Mouse strains used are described in **Table S1**.

#### *Ashcroft Scoring.*

The degree of fibrosis in the murine lung tissue was accessed by Ashcroft scoring as previously described [29].

#### *Sircol Assay.*

Collagen content was determined by Sircol Collagen Assay kit (Biocolor, Newtown Abbey, UK) as previously described [30].

#### *Flow Cytometry.*

Both murine and human flow cytometry experiments were acquired with a LSR-II flow cytometer (BD Biosciences), and information on all antibodies used in this study is listed in **Table S2**. Live cells were

gated based on forward and side scatter properties, and surface staining of cells was performed as previously described [31]. Th17 cells were identified by flow cytometry using key transcriptional factors, such as STAT3, as previously described [32]. Cells were gated on singlets, live CD3+ and CD4+ cells. Data analysis was performed using FlowJo software (Tree Star, Ashland, OR). A minimum of 50,000 events were acquired per sample.

*In Vivo Implantation of hormone pellets to ovariectomized mice.*

Ovariectomy or sham surgeries were conducted at three weeks of age by the Jackson Laboratory, and experiments were carried out when ovariectomized or sham-operated mice were 6 weeks old. At 6 weeks of age, 60-day slow-release pellets (Innovate Research of America) containing 17 $\beta$ -estradiol 0.1 mg (E2), progesterone 25 mg (P4), or a combination of 17 $\beta$ -E2 (0.1 mg) and P4 (25 mg) were surgically placed subcutaneously into ovariectomized C57BL/6J mice as previously described [33]. As a control, 25.1 mg of vehicle pellets (Innovative Research of America) were surgically placed into sham-operated females, or ovariectomized female mice. Three weeks (21 days) after pellets were implanted, mice were challenged with intranasal bleomycin (0.04 Units) and sacrificed 14 days later as previously described [34]. Studies involving large and independent experimental cohorts of mice were performed at least twice.

*Metagenomic sequencing and analysis of gut microbiota*

Fecal pellets were collected from female mice in each housing cohort and genomic DNA (gDNA) was extracted with the Qiagen DNAeasy extraction kit (Qiagen, Valencia, CA) according to the manufacturer's instructions. The gDNA concentration and quality were confirmed using the Bioanalyzer 2100 system (Agilent, Santa Clara, CA). Metagenomic sequencing of fecal pellets is detailed as previously described [39]. Sequence of gut microbiota have been deposited into BioProject ID PRJNA899808. Wilcoxon Rank Sum tests in R were used to examine differences in Shannon diversity and evenness between the ABSL-

1 and ABSL-2 environments. Code for all analyses can be found at  
[github.com/emallott/PulmonaryFibrosisMicrobiota](https://github.com/emallott/PulmonaryFibrosisMicrobiota).

## Statistics

When comparing different experimental groups, we used an unpaired two-tailed Student *t* test. Multiple-group comparisons were performed using a one-way analysis of variance (ANOVA) with Tukey's post hoc test. Statistical analysis for all figures was carried out using Prism version 7.02 (GraphPad Software). For a result to be considered statistically significant, a *P* value of less than 0.05 was used.

## 3. Results

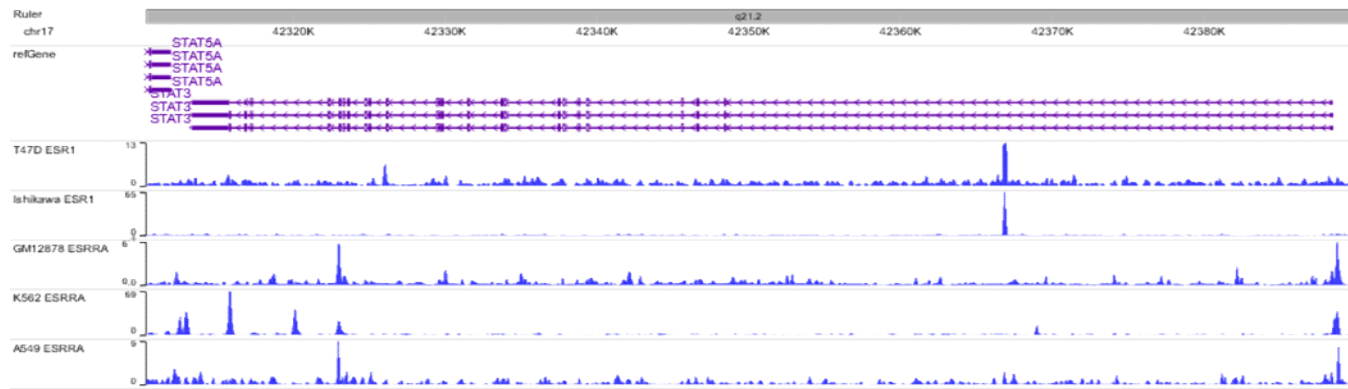
### 3.1 *The nuclear transcription factor, estrogen receptor alpha subunit, interacts with the STAT3 gene locus in CD4+ T cells*

The estrogen receptor alpha subunit (ER $\alpha$ ) is not only a receptor but also serves as a transcription factor. To identify factors that may be modulating *STAT3* expression during lung fibrosis, we interrogated ChIP-seq datasets in the ENCODE 3 repository [35]. In 5 human cell lines, including cancers and EBV-transformed B lymphocytes, significant enrichment of ER $\alpha$  binding was demonstrated within the *STAT3* locus. Representative tracks among the technical replicates for each cell line were visualized in the WashU Epigenome Browser [36] (Figure 1A). The number of starting reads, decontaminated reads, alignment success, and number of enriched peaks are given in Table S3. These findings in Chip-seq datasets confirmed previous reports that ER $\alpha$ , which is encoded by the *ESR1* gene, and *STAT3* are important in breast and ovarian cancer [18, 37], supporting the hypothesis that the *STAT3* gene locus is a frequent target of ER $\alpha$  activity in a variety of cell types.

Targeting of ER $\alpha$  to the *STAT3* gene locus in T cells has not been previously described. To determine whether ER $\alpha$  interacts with the *STAT3* locus in CD4+ T cells through DNA binding activity, we performed genome-wide ChIP-seq for ER $\alpha$  bound regions. Primary CD4+ T cells were derived from PBMCs of 6 healthy individuals with varying demographics (**Table S4**). Of the 6 ChIP libraries, four females and two males, sample p1035928-8 which corresponds to a female, identified over 6-fold greater number of ER $\alpha$ -enriched regions relative to any other sample. We used algorithm GREAT to perform ontology-based functional enrichment analyses in that sample. ER $\alpha$ -enriched sites were statistically significantly enriched in genes related to T-cell function and development (**Table S5**), suggesting that peaks obtained from this ChIP capture are specific to CD4+ T-cell function and are not randomly organized across the genome.

Finally, we examined the *STAT3* locus in detail. We found that sample p1035928-8 contains 6 ER $\alpha$ -binding regions within or proximal to the *STAT3* genomic locus, including two in its promoter region (Figure 1B). Overlaying chromatin accessibility data from the ENCODE project [35], we noted that each of these regions exhibits DNase hypersensitivity in at least one ENCODE cell line. Three of these regions also displayed evidence of estrogen-related receptor alpha (ESRRA) binding in other cell lines (K562, GM12878). Taken together, these results demonstrate that ER $\alpha$  binds the *STAT3* locus in CD4+ T cells, specifically at known regions of chromatin accessibility shared with a variety of cell types.

**A**



**B**

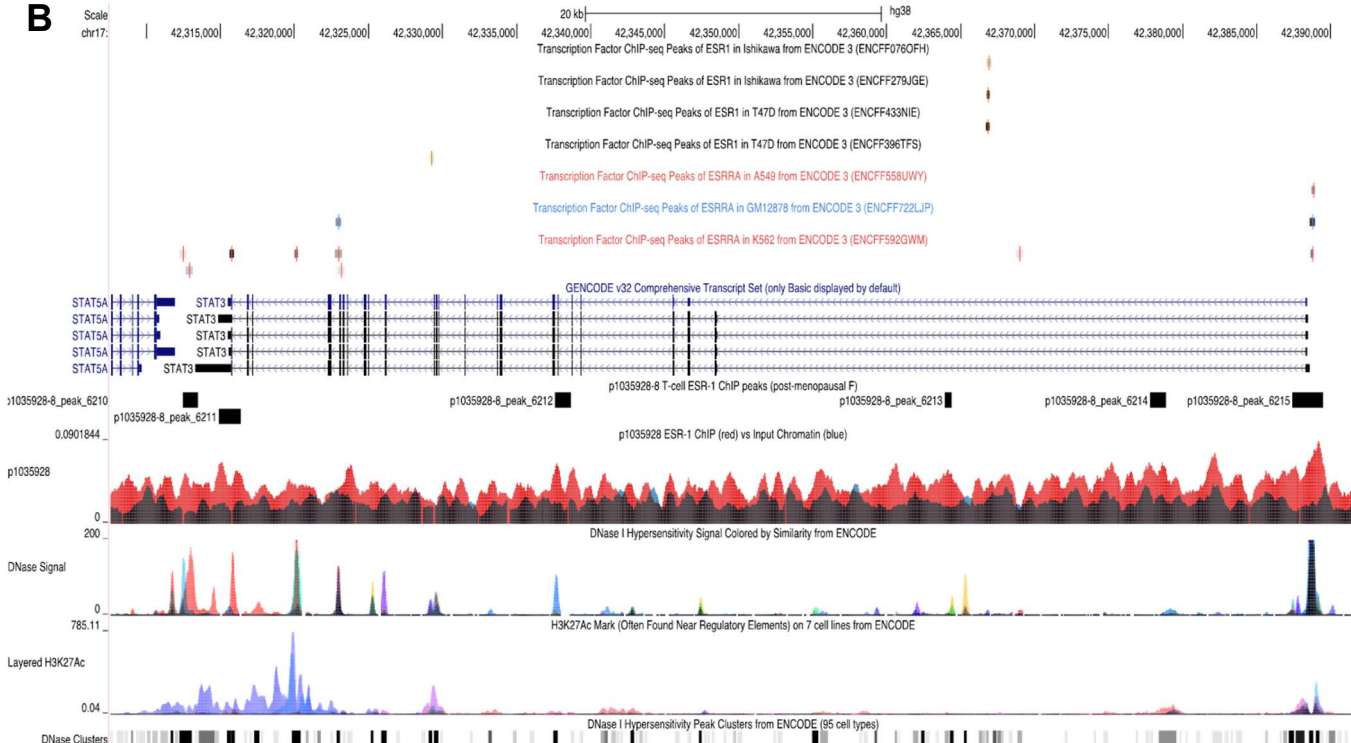


**Figure 1. Genomic visualization of ERα or ESRRA binding activity at the STAT3 gene locus. A)** Gene annotations indicate the position of STAT3, its exons (thick bars) and introns (connecting arrows, showing the direction of translation). Blue tracks indicate enrichment of ChIP-seq signal for ESR1 or ESRRA binding over background input for 5 cell lines. Sharp, prominent peaks provide evidence for the ability of these transcription factors to bind STAT3, demonstrating their interaction in these cell types. **B)** Track visualization of ERα ChIP-seq for the STAT3 locus. Primary CD4+ T-cell ERα ChIP enrichment signal (red) is depicted against input chromatin signal (black). Rectangular regions above the ChIP track indicate regions significantly enriched with ERα binding. Top: Additional tracks indicate positions of ESR1 or ESRRA binding activity in ChIP-seq data from the ENCODE project. Note that ERα binding events are not typically shared from experiment to experiment, even when cell lines are identical. Bottom: DNase and H3K27ac signal from the ENCODE project indicating regions of strong enhancer activity in general cell lines. ERα-binding regions in T-cells occur in areas with known chromatin accessibility.

### **3.2 Loss of the ESR-1 subunit represses IL-6 expression but augments pSTAT3 and IL-17A expression in CD4+ T cells**

Because the transcription factor ESR-1 (alpha subunit of ESR) was identified as binding to the *STAT3* gene in CD4+ T cells, we investigated the role of ER $\alpha$  subunit on profibrotic cytokine expression using a murine model of bleomycin-induced lung fibrosis in WT and *ESR-1* knockout (*ESR-1*<sup>-/-</sup>) mice. Both murine cohorts were challenged intranasally with bleomycin and harvested on day 14. *ESR-1*<sup>-/-</sup> mice contain supernormal estrogen levels in their serum, due to loss of the ESR-1 signaling-mediated negative feedback loop [38]. We observed that female *ESR-1*<sup>-/-</sup> mice lost significantly less weight and had the same mortality compared to their WT counterparts (Figure 2A, B). Male *ESR-1*<sup>-/-</sup> mice also demonstrated reduced weight loss but had significantly increased survival compared to WT males (Supplemental Figure 1[Figure S1]). We used flow cytometry to examine profibrotic cytokine expression in pulmonary CD4+ T cells of the murine cohorts. Levels of IL-6 and IL-23R, key mediators of Th17 cell differentiation, were significantly reduced in lung CD4+ T cells of female *ESR-1*<sup>-/-</sup> mice compared to their WT counterparts (Figure 2C, D). Remarkably, levels of pSTAT3 and IL-17A were increased in *ESR-1*<sup>-/-</sup> compared with WT mice (Figure 2E, F). These data demonstrate that ESR-1 has a key role in the induction of IL-6 and IL-23R expression in CD4+ T cells, as well as the repression of pSTAT3 and IL-17A expression in CD4+ T cells during pulmonary fibrosis of females.

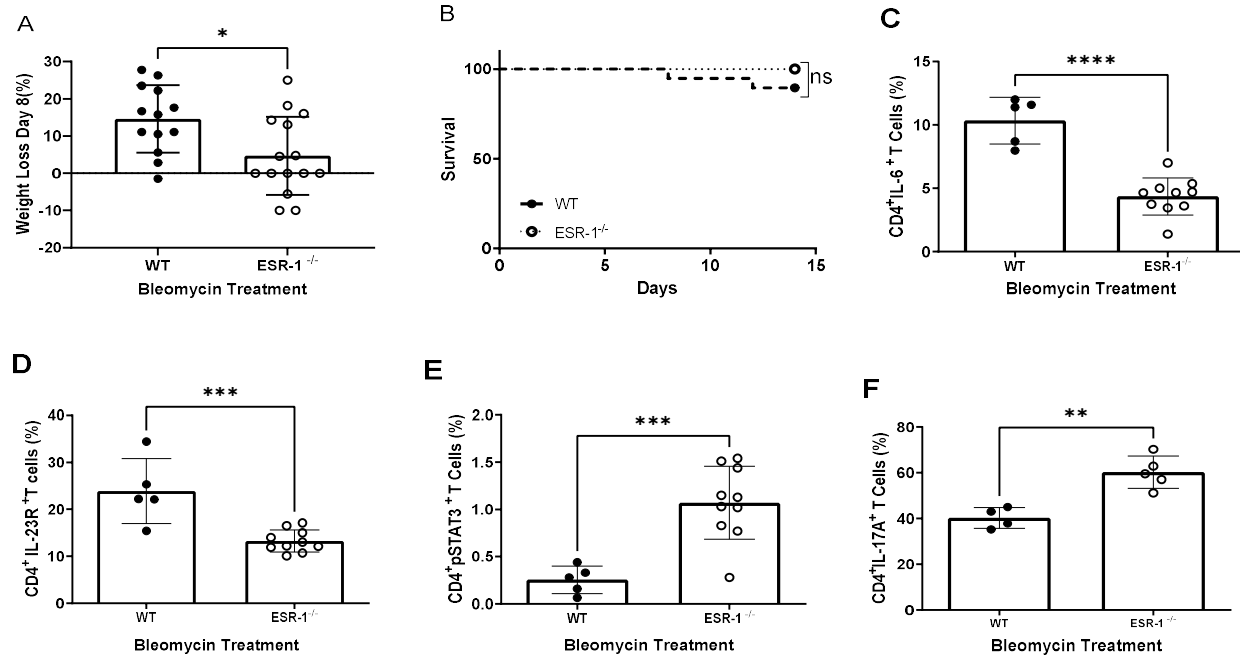


**Figure 2: Loss of estrogen receptor alpha subunit (ESR-1) improves survival and ameliorates fibrosis in female mice.** WT and ESR-/- mice were treated with bleomycin and monitored for 14 days. **A)** Body weights of mice at day 8 compared to day 0; **B)** Murine mortality across 14 days. Kaplan-Meier survival analysis with log-rank test was used to determine differences between groups. Flow cytometric analysis of T cells from single cell lung suspensions at day 14 for **C)** IL-6, **D)** IL-23R, **E)** pSTAT3Y<sup>705</sup>, and **F)** IL-17A. Comparisons between cohorts were performed using one-way ANOVA with Tukey's post-hoc. \*P < 0.05, \*\*P < 0.01, \*\*\*P < 0.001, ns: no significance. Bars are mean ± SD; each symbol represents an individual mouse. WT: Wildtype, ESR-1<sup>-/-</sup> estrogen receptor alpha knockout mice. N= 4-15

### 3.3 Loss of gonadotrophic hormones through ovariectomy reduces IL-6 production and augments

#### pSTAT3 and IL-17A expression from CD4<sup>+</sup> T cells

To further delineate the contribution of female gonadotrophic hormonal signaling to the progression of proinflammatory cytokine expression in the lung, we used female C57BL/6J mice that were ovariectomized or sham-operated at three weeks of age. Slow-release pellets containing either 17 $\beta$ -estradiol (17 $\beta$ -E2, 0.1mg), progesterone (P4, 25mg), the combination of 17 $\beta$ -E2 (0.1mg) and P4 (25mg), or vehicle (25.1mg) were subcutaneously implanted into adult ovariectomized female C57BL/6J mice at six weeks of age. At nine weeks of age, all groups were challenged with bleomycin and lungs were

harvested 14 days later. There was no significant difference in weight loss or survival across the hormone treatment groups compared to the ovariectomized mice implanted with placebo pellets (Figure 3A, B).

We performed flow cytometric analysis of single cell lung suspensions (SCLS) for alterations of CD4+ T cell populations. TGF- $\beta$  and IL-17A are profibrotic cytokines that are expressed by regulatory T cells and Th17 cells, respectively. We began by comparing regulatory T and Th17 cell populations in sham-operated, menstruating female mice. We noted a significantly higher population of regulatory T cells, compared to Th17 cells in sham-operated mice (Figure 3C). We then assessed for IL-17A cytokine expression in response to loss of female hormones. Ovariectomized mice displayed decreased CD4+IL-6+ T cells compared to sham-operated mice; supplementation with both 17 $\beta$ -E2 and P4 in ovariectomized mice normalized IL-6 expression. Neither hormone individually restored IL-6 expression by CD4+T cells to the same levels as the sham-operated mice (Figure 3D). The same trends held for the IL-6 co-receptor GP130 (Figure 3E). Remarkably, and akin to our observation in ESR-1 $^{-/-}$  mice, levels of pSTAT3 were increased in CD4+ T cells of ovariectomized mice compared to sham-operated animals, again returning to sham levels in ovariectomized mice by the addition of female hormones (Figure 3F). In accordance with an increase in pSTAT3, we also observed heightened CD4+IL-17A+ T cells in ovariectomized mice compared to sham-operated animals. Addition of 17 $\beta$ -E2, P4, or both to ovariectomized mice decreased IL-17A expression compared to placebo (Figure 3G). A representative FACS plot is provided (Figure 3H). Overall, these findings reveal that female hormones repress inflammatory profibrotic cytokine expression by inhibiting pSTAT3 signaling and IL-17A expression in murine pulmonary CD4+ T cells following bleomycin administration.

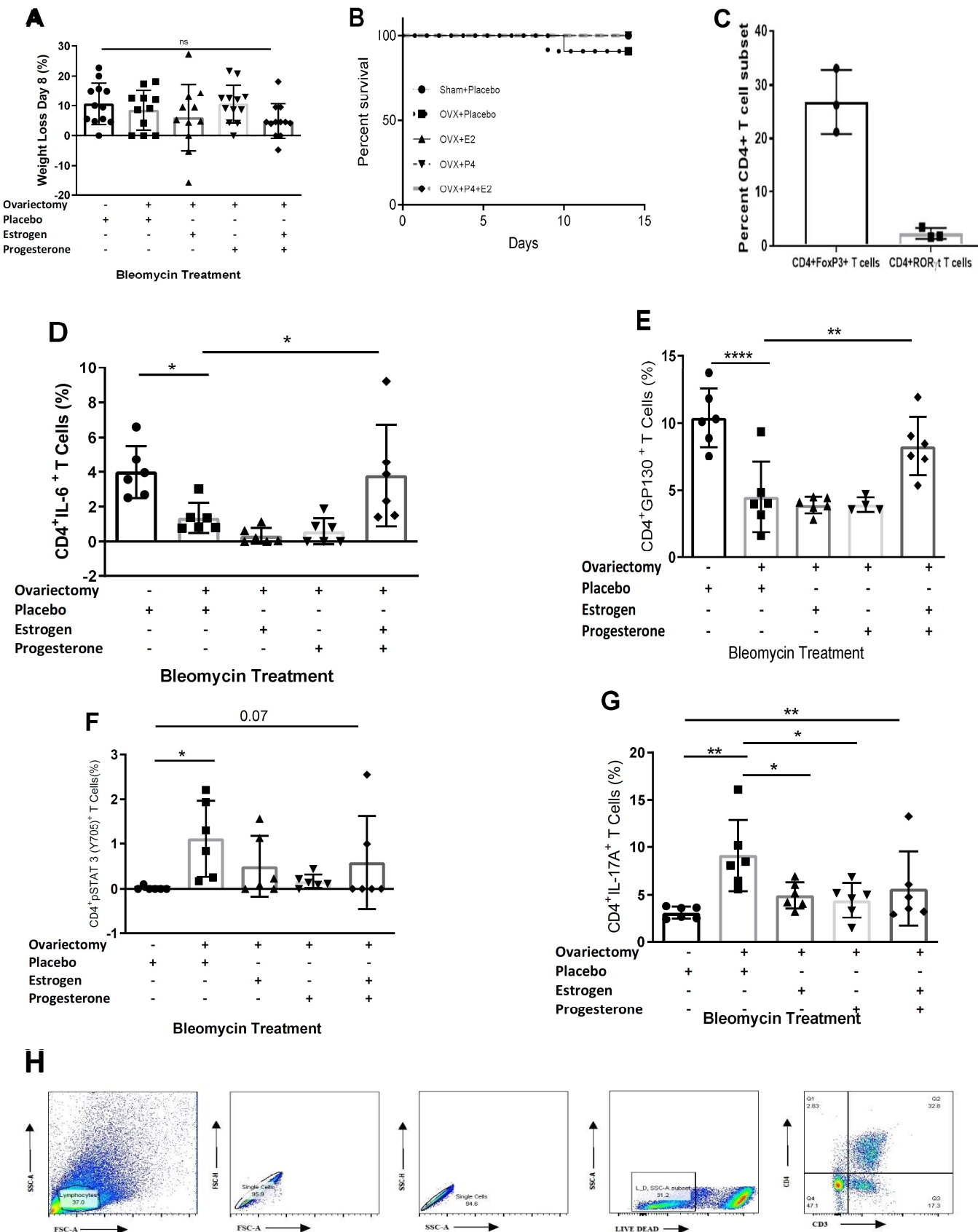


**Figure 3: In vivo administration of female hormones increases profibrotic cytokine expression in ovariectomized mice.** Hormone-containing or placebo pellets were implanted into ovariectomized C57BL/6 female mice for 21 days, followed by bleomycin administration and monitored for an additional 14 days. **A)** Body weights of mice at day 8 after bleomycin administration; **B)** Murine mortality across 14 days; **C)** Flow cytometric analysis of T cells from single cell lung suspensions for **D) IL-6, E) GP130, F) pSTAT3Y<sup>705</sup> and G) IL-17A. H)** Representative FACS plots illustrating CD4+ percentage in bleomycin-treated murine cohorts. Comparisons between cohorts were performed using one-way ANOVA with Tukey's post-hoc. \*P < 0.05, \*\*P < 0.01, \*\*\*\*P < 0.0001. ns: no significance RLL: right lower lobe. Bars are mean ± SD; each dot represents an individual mouse. N=3-12 per cohort.

### 3.4 Lung quantification following loss of ESR-1 or ovariectomy reveals reduced collagen content

To determine the physiologic significance of estrogen signaling on profibrotic cytokine expression, we performed histologic analysis, as well as collagen quantification of the lung using the Sircol assay. Analysis of lung histology using trichrome staining noted significantly less fibrosis in ovariectomized mice without hormone replacement compared to sham-operated mice or ovariectomized mice given dual estrogen (17 $\beta$ -E2)/progesterone (P4) hormone pellets (Figure 4A). Ashcroft scoring (Figure S2) and quantification of collagen content (Figure 4B) revealed a nonsignificant decrease in collagen levels in ovariectomized mice compared to mice with sham ovariectomy surgeries. Replacement of female hormones with a combination of estrogen and progesterone pellets increased fibrosis compared to the ovariectomized placebo group (Figure 4B). Similarly, a non-significant decrease in pulmonary collagen content was observed in ESR-1/- mice compared to wild-type mice. The observation of a nonsignificant decline in pulmonary lung content following loss of estrogen signaling suggests that additional factors contribute to pathogenesis. We recently reported that gut microbiota play an important role in lung fibrosis severity. ABSL-1 housing conditions favor gut microbiota diversity, whereas ABSL-2 conditions favor reduced gut microbiota diversity [39]. Using linear discriminant analysis (LDA) to examine species-level differences in the gut microbiota, 10 taxa were overrepresented in ABSL-1 mice and 5 taxa were overrepresented in ABSL-2 mice. The overrepresented taxa in ABSL-2 mice included *Lachnospiraceae bacterium A2*, *Lachnospiraceae bacterium 28-4*, *Firmicutes bacterium ASF500*, and *Romboutsia ilealis* [39]. Higher relative abundance of Firmicutes in the lung microbiota of bleomycin-

treated mice with fibrosis has been reported[40]. Species overrepresented in ABSL-1 mice included *Staphylococcus nepalensis*, *Dubosiella newyorkensis*, *Acetatifactor muris*, *Lactobacillus animalis*, *Lactobacillus murinus*, and *Acutalibacter muris* [39].

No distinctions in the lung microbiota are present in these mice by housing condition. Specifically, rearing environments that favor low gut microbiota diversity, such as ABSL-2 housing conditions, induce severe lung disease compared to ABSL-1 conditions. To confirm if gut microbiota impact female ILD severity, we began by assessing lung collagen content in wild-type female mice who received intranasal bleomycin while housed in different environments: germ-free, ABSL-1 or ABSL-2 conditions. We noted significant distinctions in lung collagen content among wild-type females according to rearing environment, with ABSL-2 female mice demonstrating the most severe disease, compared to germ-free or ABSL-1 mice (Figure 4D). To determine the impact of estrogen signaling and gut microbiota on lung fibrosis severity, we assessed lung collagen content among ovariectomized mice, as well as those ovariectomized with estrogen replacement, while housed in either ABSL-1 or ABSL-2 conditions. Remarkably, we noted that ovariectomized mice housed in ABSL-1 or ABSL-2 conditions did not demonstrate a change in collagen content (Figure 4E). Equally noteworthy was the observation that a significant increase in lung fibrosis was noted among ovariectomized mice who received estrogen replacement and were housed in ABSL-2 conditions compared to those housed in ABSL-1 conditions. These findings reveal a synergistic relationship of estrogen signaling and gut dysbiosis on lung fibrosis severity (Figure 4E).

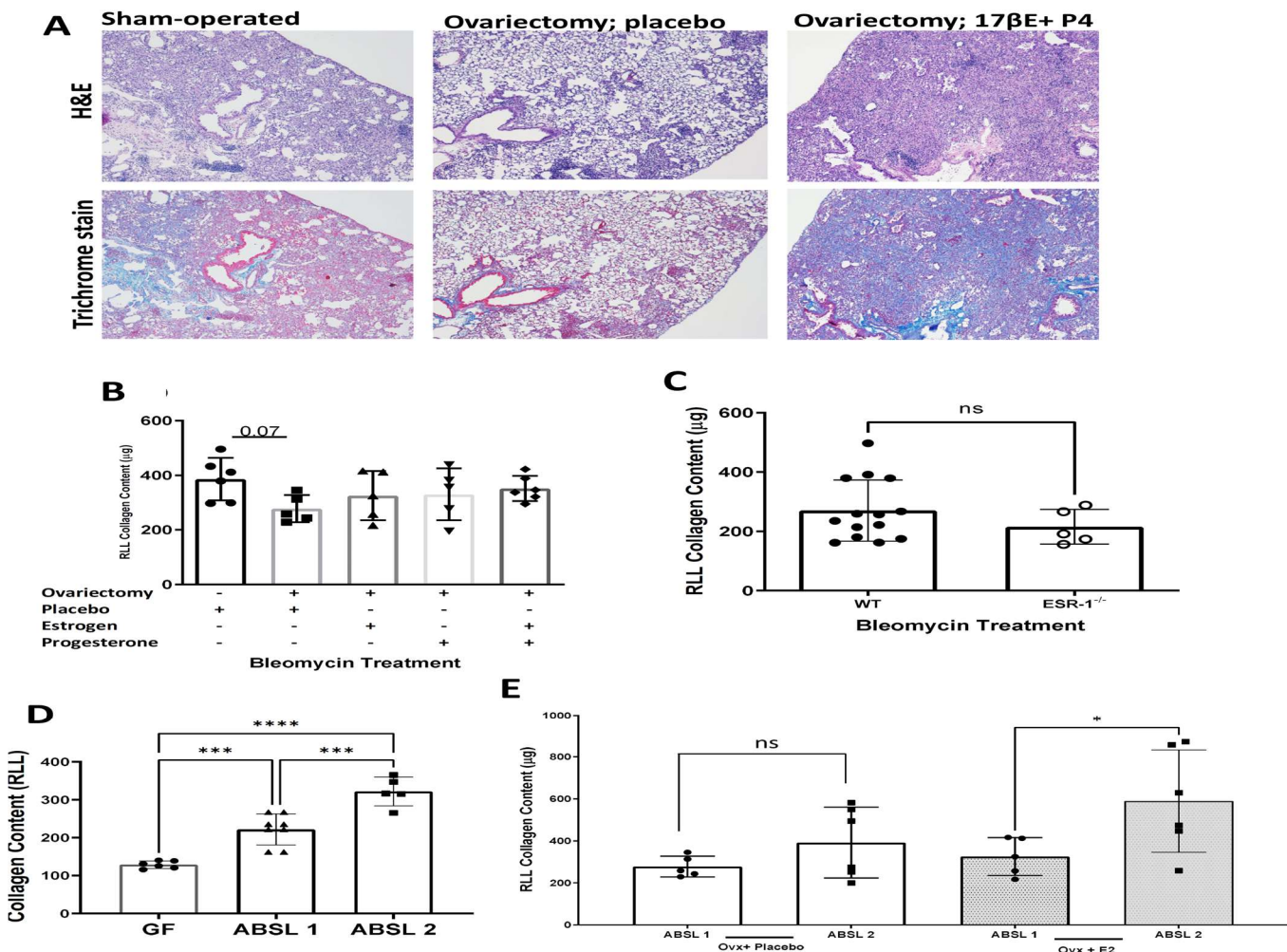


**Figure 4. Quantification of bleomycin-induced pulmonary collagen quantification with various hormone deletion or repletion conditions in distinct housing environments.** A) Representative H&E and trichrome histologic stains of lungs at day 14 under various hormone conditions; B) Pulmonary collagen quantification of lung under baseline, hormone depletion and hormone repletion conditions. C) Pulmonary collagen quantification of lung under wild-type (WT) and ESR1 null conditions; D) Pulmonary collagen quantification in menstruating female mice housed in germ-free, ABSL-1 and ABSL-2 environments; E) Pulmonary collagen quantification of ovariectomized and estrogen-repleted mice in ABSL-1 and ABSL-2 environments. Comparisons between cohorts were performed using one-way ANOVA with Tukey's post-hoc. \*P < 0.05, \*\*\*P < 0.001, \*\*\*\*P < 0.0001. ns: no significance RLL: right lower lobe. Bars are mean ± SD; each dot represents an individual mouse. N=5-14.

### **3.5 Female gut microbiota demonstrate significantly less diversity in ABSL-2 housing conditions**

To investigate the hypothesis that the gut microbiota is an important contributor to the differences in fibrosis severity between female mice housed under ABSL-1 and ABSL-2 conditions, we performed

metagenomic analysis on fecal pellets from female mice in each housing cohort. We did not detect microorganisms in the stool of female germ-free mice by sequencing and culture, as expected. Shannon alpha diversity, a measure of species richness and evenness, was considerably higher in female ABSL-1 mice compared with female ABSL-2 mice using a Wilcoxon rank sum test (Figure 5A). Additionally, Pielou's evenness was higher in ABSL-1 compared with ABSL-2 female mice, but species richness did not differ significantly (Shannon diversity: Wilcoxon,  $W=108$ ,  $p=0.015$ ; Pielou's evenness: Wilcoxon,  $W=106$ ,  $p=0.021$ ; Species richness: Wilcoxon,  $W=80.5$ ,  $p=0.450$ ). Female mice housed under ABSL-1 and ABSL-2 conditions differed significantly in their gut microbiome composition using Jaccard, but not Bray-Curtis, dissimilarities (PERMANOVA, Bray-Curtis:  $F_{1,22}=2.392$ ,  $R^2=0.098$ ,  $p=0.079$ ; Jaccard:  $F_{1,22}=8.369$ ,  $R^2=0.276$ ,  $p<0.001$ ). A similar investigation in male mice revealed that the ABSL-1 and ABSL-2 microbiomes were significantly different using both metrics (PERMANOVA, Bray-Curtis:  $F_{1,24}=4.728$ ,  $R^2=0.165$ ,  $p=0.004$ ; Jaccard:  $F_{1,24}=6.519$ ,  $R^2=0.214$ ,  $p<0.001$ ) (Figure S4). Alpha diversity did not differ significantly between floors for male individuals (all  $p>0.05$ ).

Comparison of female and male gut microbiota diversity according to housing conditions reveals significantly greater gut diversity among females, compared to males, in ABSL-1 housing conditions (Figure 5B); whereas, only greater species richness was noted among females in ABSL-2 housing conditions (Figure 5C). Beta diversity differences between ABSL-1 and ABSL-2 microbiota compositions also differed significantly when analysis was conducted using both the Bray-Curtis dissimilarity metric index (Figure 5D) and Jaccard index (Figure 5E) that account for presence/absence of taxa and taxon abundance variation, respectively (PERMANOVA, ABSL-1 mice: Bray-Curtis:  $F_{1,17}=4.424$ ,  $R^2=0.206$ ,  $p=0.014$ ; Jaccard:  $F_{1,17}=2.408$ ,  $R^2=0.124$ ,  $p=0.053$ ; ABSL-2 mice: Bray-Curtis:  $F_{1,29}=1.952$ ,  $R^2=0.063$ ,  $p=0.160$ ; Jaccard:  $F_{1,29}=7.944$ ,  $R^2=0.215$ ,  $p<0.001$ ). These findings support the hypothesis that the female gut microbiome changes according to rearing environment.

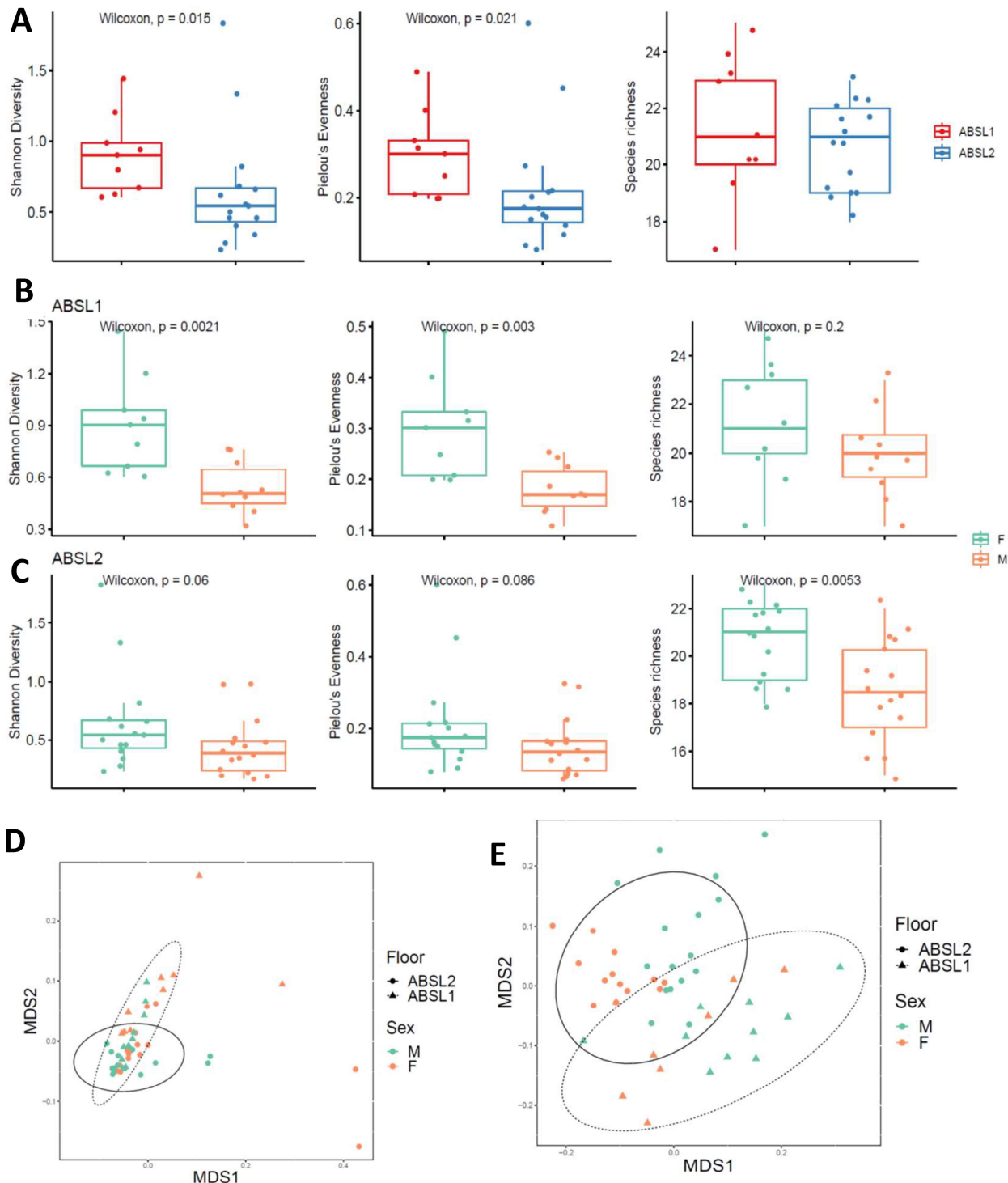


**Figure 5. Murine female gut microbial diversity is modified by housing environment.** **A)** Shannon diversity index, Pielou's evenness and species richness scores for female mice housed in ABSL-1 and ABSL-2 facilities following bleomycin inoculation ( $n=9\text{-}14$  mice per cohort). The boxes show the median, as well as the 25th and 75th quartiles. The whiskers extend to  $1.5 \times \text{IQR}$ . Each dot represents one mouse. **B, C)** Comparison of female and male Shannon diversity index, Pielou's evenness and species richness scores for female mice housed in ABSL-1 and ABSL-2 facilities following bleomycin inoculation ( $n=14\text{-}16$  mice per cohort). **D)** Nonlinear multidimensional scaling (MDS) plot showing differences in microbial taxonomic composition based on Jaccard dissimilarity. **E)** Nonmetric multidimensional scaling plot based on Bray-Curtis and Jaccard dissimilarity showing the gut microbiome by gender of murine communities housed on ABSL1 and ABSL2 floors.

### **3.6 Patients with progressive fibrotic lung disease display sex-specific profibrotic cytokine profiles**

Because of the role of female gonadotrophic hormones in reducing the CD4+ T cell-mediated proinflammatory, profibrotic environment in mouse models of lung fibrosis, we probed samples from human patients with fibrotic lung diseases for sex-associated differences. Consistent with the murine model of lung fibrosis, we observed higher levels of STAT3 mRNA and pSTAT3 protein in CD4+ T cells from male compared to female sarcoidosis patients (Figure 6A, B). We noted similarly increased mRNA and protein expression of the master transcription factor regulating IL-17A production, RORC, in CD4+ T cells from male compared to female sarcoidosis patients (Figure 6C, D). Additionally, among sarcoidosis patients experiencing disease progression, females expressed significantly higher IL-6 levels in their CD4+ T cells compared to males (Figure 6E).

We also assessed for IL-17A and TGF- $\beta$ 1 production by sex, as CD4+ T cells promote pulmonary fibrosis through STAT3-mediated production of IL-17A and TGF- $\beta$ 1 [16]. We observed higher IL-17A mRNA and protein expression in CD4+ T cells from male compared to female sarcoidosis patients (Figure 6F, G). CD4+ T cells from female sarcoidosis patients expressed significantly higher free TGF- $\beta$ 1 than males and female healthy controls (Figure 6H). There were no distinctions in the TGF- $\beta$ 1 precursor protein, latency-associated peptide-TGF- $\beta$ , among males compared to females (Figure 6I). These findings demonstrate differential immune modulation of STAT3 signaling pathways in human CD4+ T cells of males (increased) and females (reduced) with fibrotic lung disease. Consequently, CD4+ T cells from males exhibit higher proinflammatory cytokine expression due to enhanced IL-17A production, whereas CD4+ T cells from females exhibit increased immunosuppressive cytokines due to greater TGF- $\beta$ 1 expression.

We assessed for a possible contribution of female hormones to other fibrotic diseases, including IPF and Systemic Sclerosis (SSc), by quantifying serum 17 $\beta$ -E2 levels in age-matched patients and healthy

controls. Serum 17 $\beta$ -E2 was greater in male SSc and IPF patients compared to age-matched male healthy controls (Figure 6J). These findings demonstrate the positive interplay of female gonadotrophic hormones in male- and female-predominant fibrotic lung diseases.

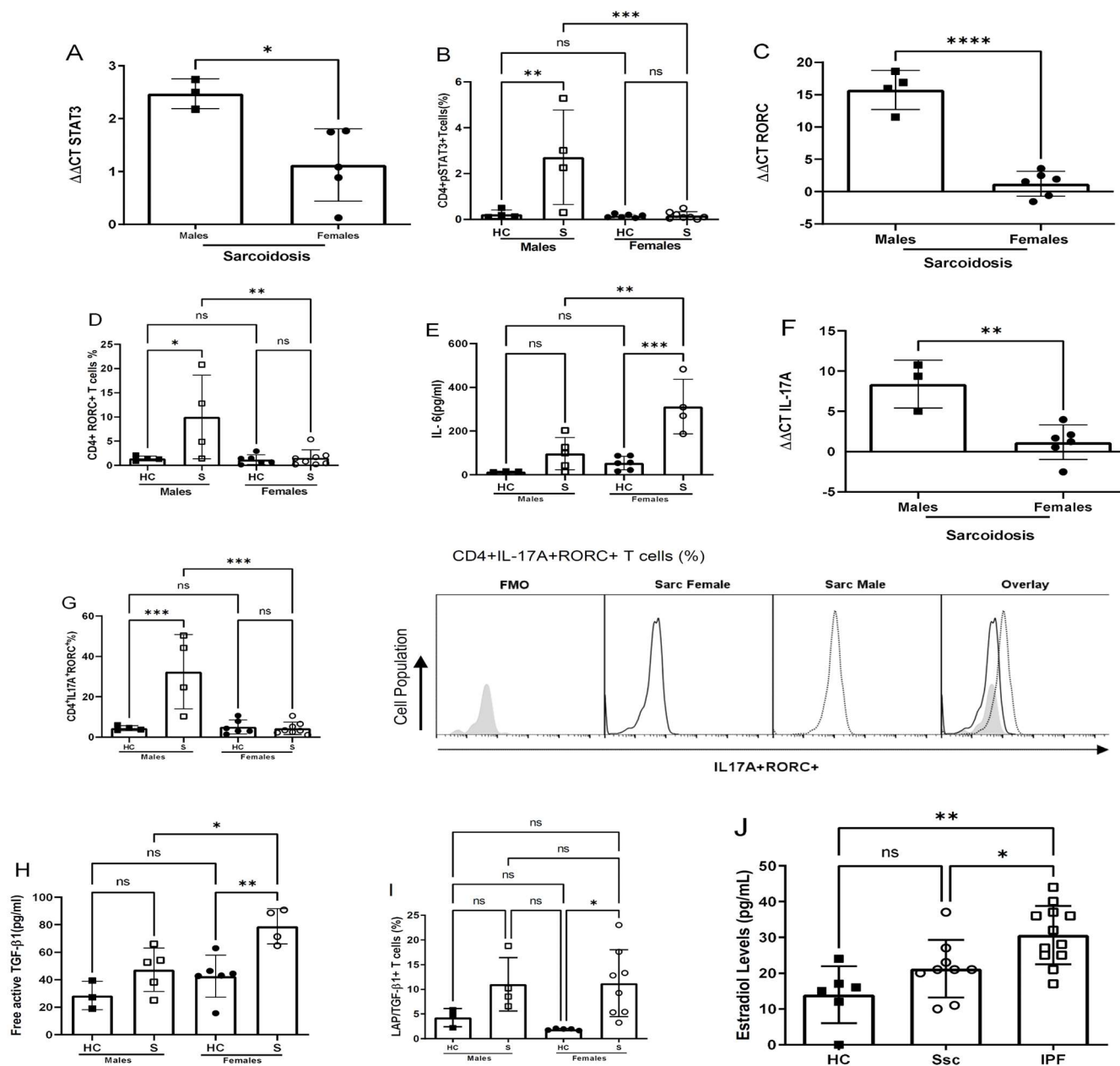


**Figure 6: Male and female sarcoidosis patients display distinct profibrotic cytokine profiles.** Purified CD4+ T cells from the peripheral blood of healthy controls and sarcoidosis patients were anti-CD3 and anti-CD28 TCR stimulated and cultured for 24 hours, followed by real time-PCR for **A) STAT3 C) RORC F) IL-17A**; flow cytometry for **B) pSTAT3Y<sup>705</sup> D) RORC G) IL-17A I) LAP/TGF- $\beta$ 1 E) cytokine bead array for IL-6 and H) enzyme-linked immunosorbent assay for free TGF- $\beta$ 1 analysis. J) Estradiol levels in serum of healthy controls, IPF, and scleroderma patients. Comparisons between cohorts were performed using one-way ANOVA with Tukey's post-hoc. Bars are mean  $\pm$  SD; each dot is an individual patient. \*P < 0.05, \*\*P < 0.01, \*\*\*P < 0.001, \*\*\*\*P < 0.0001. ns: no significance. HC: healthy controls, S: sarcoidosis, SSc: systemic sclerosis, IPF: idiopathic pulmonary fibrosis**

## Discussion

This original report reveals the “ying-yang” effects of estrogen-induced lung fibrosis in female interstitial lung disease. Estrogen clearly augments the development of lung fibrosis (Figure 4) yet the binding of ER $\alpha$  to the STAT3 promoter shifts profibrotic cytokine expression away from proinflammatory phenotypes mediated by IL-17A to immunosuppressive phenotypes mediated by TGF- $\beta$ 1 (Figures 2, 3). Human cytokine expression confirmed reduced pSTAT3 expression in females, leading to increased TGF- $\beta$ 1 production, whereas males display higher IL-17A levels.

The beneficial effects of estrogen were apparent. Although ESR-1 $^{-/-}$  mice and surgical ovariectomy confirm estrogen's profibrotic capacity in lung fibrosis, it is worth noting that Th17 cell differentiation is reduced due to the transcription factor ER $\alpha$  ability to the STAT3 promoter (Figures 1-3). Loss of STAT3 signaling has been shown to shift IL-6-JAK2-STAT3 induction of IL-17A to sustained IL-6-ERK-TGF- $\beta$ 1 expression in local and systemic CD4+ T cells [15, 16]. This is the most likely explanation for the increased regulatory T cells noted in females and the increased STAT3 signaling and IL-17A production following ovariectomy (Figure 3, 6). Both ovariectomized and ESR-1 $^{-/-}$  mice revealed significantly lower IL-6 and GP130 levels than sham-treated animals but increased pSTAT3 and IL-17A levels in CD4+ T cells (Figure 3). Higher estrogen states augment IL-6 production, but instead of inducing a proinflammatory state supported by increased CD4+ IL-17A levels, estrogen concomitantly inhibits STAT3 signaling. These immune alterations are likely relevant to other IL-17A-mediated diseases in the postmenopausal state, such as myocardial infarctions and osteoporosis [41, 42]. Enhanced TGF- $\beta$ 1 expression protects against osteoporosis [43].

The pathologic effects of estrogen were also determined. A prior study noted increased ESR-1 expression in human IPF lung samples and that chemical inhibition of ESR-1 results in reductions in bleomycin-induced pulmonary fibrosis in male mice [44]. Genetic and surgical ablation of estrogen-dependent signaling resulted in reductions in pulmonary collagen content, which confirms the profibrotic

nature of estrogen in female predominant ILD (Figures 4). Remarkably, the observed reductions were not statistically significant, suggesting that other factors contribute to lung fibrosis severity in females. Induction of lung fibrosis in females under distinct housing conditions unveiled the role of the gut microbiome to lung fibrosis severity. Wild-type female mice treated with intranasal bleomycin demonstrate the greatest lung severity in ABSL-2 conditions, and minimal fibrosis under germ-free conditions, thus confirming the important contribution of gut flora to female lung fibrosis (Figure 4D). Conditions that favor the loss of female gut microbial diversity, such as ABSL-2 housing conditions, leads to greater lung fibrosis, compared to ABSL-1 conditions (Figure 4, 5). Equally noteworthy is the observation that fibrosis is synergistic between estrogen signaling and gut dysbiosis, suggesting that the profibrotic nature of estrogen is heavily influenced by gut microbiota and that the capacity of gut microbiota to induce fibrosis is influenced by host hormone status. A growing body of literature supports crucial interactions of gut microbiota and estrogens [45, 46]. Conjugation of glucuronic acid (GlcA) to a compound, such as estrogen, marks it for elimination via the GI or urinary tract.  $\beta$ -glucuronidase, an enzyme which deconjugates estrogen, mediates estrogen release into the serum in its active form [47, 48]. Gut microbiota can inhibit or induce  $\beta$ -glucuronidase activity. In addition, it was previously noted that ABSL-2 stool contains reduced lactobacilli within the microbial community. *Lactobacillus* spp, which were elevated in ABSL-1 stool, can reduce fecal  $\beta$ -glucuronidase activity[46]; future studies that assess the capacity of lactobacilli to enhance estrogen urinary excretion and lowering its serum levels are needed. Future studies to define the mechanisms by which ABSL-2 gut flora augment estrogen induction of lung fibrosis are also warranted. Consideration of the hormone status of the host, as well as defining the gut microbiome, is necessary to explain the clinical observation in females with ILD. TGF- $\beta$ 1 is the master regulator of fibrosis. Figure 6 demonstrates that TGF- $\beta$ 1 is most predominant in female sarcoidosis patients. This reason there is more fibrosis in females is due to the increased TGF- $\beta$ 1 expression. Estrogen

signaling also provides protection against proinflammatory fibrosis due to the capacity of the ER $\alpha$  to bind to the *STAT3* promoter (Figure 1). This reduction in lung inflammation improves prognosis. In Figure 4, we see that gut dysbiosis also augments lung fibrosis. In menopausal females, the gut microbiome continues to drive lung fibrosis, but due to the reduced estrogen state, the lung fibrosis can now be mediated by IL-17A which likely explains the increased symptoms after menopause.

There are some limitations that should be noted. This investigation focused on female ILD; investigations of the role of testosterone on lung fibrosis are needed. There are also reports that estrogen drives Th17 cell differentiation in chronic lung diseases, such as asthma [49, 50]. Concomitant immune-gut microbiome investigations of asthma models with ILD models are warranted, including an inquiry of the interplay of gonadal hormones. Also, asthma pathogenesis is very distinct from ILD, which may also impact T cell differentiation. Another consideration is that the gut microbiome is influenced by diet. The mice in the murine model had the same diet; future studies to assess the impact of food consumption on the gut microbial community, metabolomic syndromes and inflammation is warranted [51-53]. Investigation of the impact of gut dysbiosis on estrogen signaling or estrogen signaling on gut microbial communities is warranted. Finally, we observed Th17 cell populations increasing following gavage of ABSL-2 stool into germ-free mice, compared to gavaging of ABSL-1 stool. Future analysis to definitively identify the microorganism(s) responsible for Th17 cell differentiation is warranted, followed by an assessment for their presence in the stool of asthma murine models, as well as asthmatic patients and ILD patients.

## Conclusions

Taken together, this investigation demonstrates that female gonadotrophic hormones are profibrotic yet, through ER $\alpha$  binding of the *STAT3* locus, reduces the inflammation induced by IL-17A expression in

CD4+ T cells. The consequent reduction in inflammation is a likely contributor to the mortality benefit observed in premenopausal females with ILD. This study introduces another key contributor to lung fibrosis severity, gut dysbiosis. The synergistic impact of gut dysbiosis and estrogen on lung fibrosis supports a multi-pronged approach to the treatment of female predominant lung fibrosis (Figure 7).

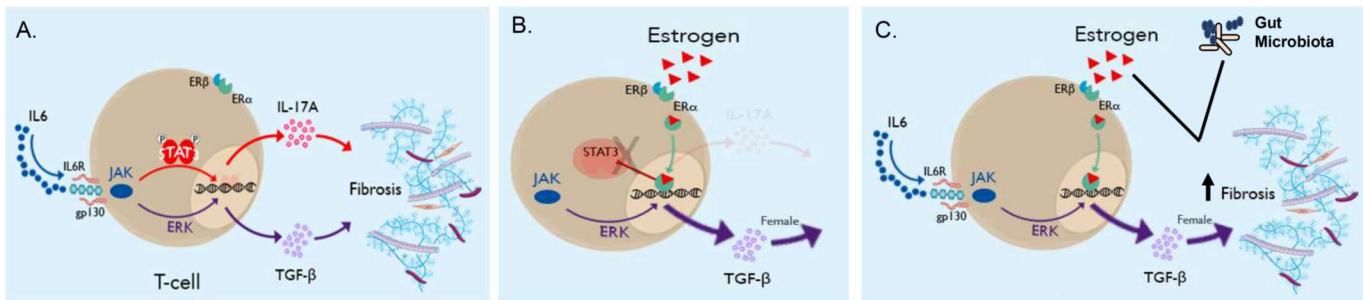


**Figure 7. Graphical abstract of gonadal hormones and gut dysbiosis interaction on lung fibrosis.**

**(A)** IL-6 induces profibrotic cytokine expression through IL-17A and TGF- $\beta$ 1 expression. IL-17A drives inflammation in fibrotic lung tissue. **(B)** The alpha subunit of the estrogen receptor (ER $\alpha$ ) serves as a transcription factor and physically binds to the *STAT3* promoter, thus inhibiting the Th17 cell-mediated inflammation associated with fibrosis. **(C)** The presence of estrogen and gut dysbiosis augments lung fibrosis, thus demonstrating that multiple factors contribute to lung fibrosis pathophysiology.

**Table 1. Demographic information of sarcoidosis, IPF, scleroderma patients and healthy control subjects used in this study.**

	<b>Healthy Control</b>	<b>Sarcoidosis</b>	<b>IPF</b>	<b>Scleroderma</b>
<b>Number</b>	25	31	45	11
<b>Gender (male, female)</b>	7,18	11,20	36, 9	5, 6
<b>Age years Median (Minimum, Maximum)</b>	44 (23,65)	50 (27,72)	66(50, 83)	60(49, 86)
<b>Race</b>	12 AA, 13 C	16 AA, 15 C	45C	7C, 3AA, 1 Asian

ILD: Interstitial Lung Disease; C: Caucasian, AA: African American, IPF: Idiopathic Pulmonary Fibrosis

### **Patents: NA**

**Supplemental Materials:** The following supporting information can be downloaded at: [www.mdpi.com/xxx/s1](http://www.mdpi.com/xxx/s1), Figure S1, S2 and S3, as well as Supplemental Table 1-5.

### **Author Contributions**

W.P.D. conceived the study; W.P.D., O.S.C., and D.C.N. designed the experiments; Experiments were performed, validated and analyzed by O.S.C., E.M., D.W., M. L., A.L., B.S-G., H.W., N.C., J.E.J., C.G.M., and E.M.W.; Drafting the manuscript for important intellectual content was done by S.B., E.M., O.S.C., B.S-G., A.G., L.L., C.G.M., L.V.K., D.C.N., and W.P.D. All authors have read and agreed to the published version of the manuscript.

## Funding

O.S.C.: Foundation for Sarcoidosis Research (FSR) Fellowship Program 17-904, T32 AR059039-10;  
W.P.D.: Ellen Dreiling Research Fund Endowment and the Vanderbilt Microbiome Initiative; FSR 19-505-SGP, HL117074, K24 HL127301 and K24 HL127301-1S; Z.W.: 5 T32 HL094296; C.G.M.: NHLBI R01HL113326-06, NIGMS P30 GM110766-01; D.C.N.: R01 HL122554; L.V.K.: R01 AI139046; E.M.W.: T32HL087738; N.C. T32GM007347.

## Institutional Review Board Statement

This study was conducted in accordance with the Declaration of Helsinki and approved by the Institutional Review Board of Vanderbilt University Medical Center.

## Informed Consent Statement

Informed consent was obtained from all subjects involved in the study.

## Data Availability Statement

All sequences obtained from the lung and gut microbiome analysis of germ-free, ABSL-1 and ABSL-2 mice has been deposited into BioProject ID, Accession number PRJNA899808.

## Code Availability Statement

Code for all analyses can be found at [github.com/emallott/PulmonaryFibrosisMicrobiota](https://github.com/emallott/PulmonaryFibrosisMicrobiota).

## Acknowledgements

We gratefully acknowledge sarcoidosis, IPF and Ssc patients for their willingness to further research through study participation, and clinical providers, including Robert P. Baughman, who helped identify patients.

**Conflict of interest statement:** L. Van Kaer is a member of the scientific advisory board of Isu Abaxis Co., Ltd. (South Korea). The other authors have declared that no conflict of interest exists.

## References

- [1] M. A. Carey, J. W. Card, J. W. Voltz, D. R. Germolec, K. S. Korach, and D. C. Zeldin, "The impact of sex and sex hormones on lung physiology and disease: lessons from animal studies," *Am J Physiol Lung Cell Mol Physiol*, vol. 293, no. 2, pp. L272-8, Aug 2007, doi: 10.1152/ajplung.00174.2007.
- [2] P. Pandit, R. L. Perez, and J. Roman, "Sex-Based Differences in Interstitial Lung Disease," *Am J Med Sci*, vol. 360, no. 5, pp. 467-473, Nov 2020, doi: 10.1016/j.amjms.2020.04.023.
- [3] D. Yang *et al.*, "Dysregulated Lung Commensal Bacteria Drive Interleukin-17B Production to Promote Pulmonary Fibrosis through Their Outer Membrane Vesicles," *Immunity*, vol. 50, no. 3, pp. 692-706 e7, Mar 19 2019, doi: 10.1016/j.jimmuni.2019.02.001.
- [4] S. Downs-Canner *et al.*, "Suppressive IL-17A(+)Foxp3(+) and ex-Th17 IL-17A(neg)Foxp3(+) T(reg) cells are a source of tumour-associated T(reg) cells," *Nat Commun*, vol. 8, p. 14649, Mar 14 2017, doi: 10.1038/ncomms14649.
- [5] L. J. Celada *et al.*, "Programmed Death-1 Inhibition of Phosphatidylinositol 3-Kinase/AKT/Mechanistic Target of Rapamycin Signaling Impairs Sarcoidosis CD4(+) T Cell Proliferation," *Am J Respir Cell Mol Biol*, vol. 56, no. 1, pp. 74-82, Jan 2017, doi: 10.1165/rcmb.2016-0037OC.
- [6] M. K. Han *et al.*, "Female Sex and Gender in Lung/Sleep Health and Disease. Increased Understanding of Basic Biological, Pathophysiological, and Behavioral Mechanisms Leading to Better Health for Female Patients with Lung Disease," *Am J Respir Crit Care Med*, vol. 198, no. 7, pp. 850-858, Oct 1 2018, doi: 10.1164/rccm.201801-0168WS.
- [7] M. T. Durheim *et al.*, "In-Hospital Mortality in Patients with Idiopathic Pulmonary Fibrosis: A US Cohort Study," *Lung*, vol. 197, no. 6, pp. 699-707, Dec 2019, doi: 10.1007/s00408-019-00270-z.
- [8] A. L. Olson, J. J. Swigris, D. C. Lezotte, J. M. Norris, C. G. Wilson, and K. K. Brown, "Mortality from pulmonary fibrosis increased in the United States from 1992 to 2003," *Am J Respir Crit Care Med*, vol. 176, no. 3, pp. 277-84, Aug 1 2007, doi: 10.1164/rccm.200701-044OC.
- [9] W. Jacobs *et al.*, "The right ventricle explains sex differences in survival in idiopathic pulmonary arterial hypertension," *Chest*, vol. 145, no. 6, pp. 1230-1236, Jun 2014, doi: 10.1378/chest.13-1291.
- [10] K. M. Olsson *et al.*, "Anticoagulation and survival in pulmonary arterial hypertension: results from the Comparative, Prospective Registry of Newly Initiated Therapies for Pulmonary Hypertension (COMPERA)," *Circulation*, vol. 129, no. 1, pp. 57-65, Jan 7 2014, doi: 10.1161/CIRCULATIONAHA.113.004526.
- [11] J. J. Swigris *et al.*, "Sarcoidosis-related mortality in the United States from 1988 to 2007," *Am J Respir Crit Care Med*, vol. 183, no. 11, pp. 1524-30, Jun 1 2011, doi: 10.1164/rccm.201010-1679OC.
- [12] M. S. Wilson *et al.*, "Bleomycin and IL-1beta-mediated pulmonary fibrosis is IL-17A dependent," *J Exp Med*, vol. 207, no. 3, pp. 535-52, Mar 15 2010, doi: 10.1084/jem.20092121.
- [13] D. Chakraborty *et al.*, "Activation of STAT3 integrates common profibrotic pathways to promote fibroblast activation and tissue fibrosis," *Nat Commun*, vol. 8, no. 1, p. 1130, Oct 24 2017, doi: 10.1038/s41467-017-01236-6.
- [14] S. Ahmed, D. P. Misra, and V. Agarwal, "Interleukin-17 pathways in systemic sclerosis-associated fibrosis," *Rheumatol Int*, vol. 39, no. 7, pp. 1135-1143, Jul 2019, doi: 10.1007/s00296-019-04317-5.
- [15] C. A. Fielding *et al.*, "Interleukin-6 signaling drives fibrosis in unresolved inflammation," *Immunity*, vol. 40, no. 1, pp. 40-50, Jan 16 2014, doi: 10.1016/j.jimmuni.2013.10.022.
- [16] L. J. Celada *et al.*, "PD-1 up-regulation on CD4(+) T cells promotes pulmonary fibrosis through STAT3-mediated IL-17A and TGF-beta1 production," *Sci Transl Med*, vol. 10, no. 460, Sep 26 2018, doi: 10.1126/scitranslmed.aar8356.
- [17] D. Kamimura, K. Ishihara, and T. Hirano, "IL-6 signal transduction and its physiological roles: the signal orchestration model," *Rev Physiol Biochem Pharmacol*, vol. 149, pp. 1-38, 2003, doi: 10.1007/s10254-003-0012-2.

- [18] J. H. Ma *et al.*, "STAT3 Targets ERR-alpha to Promote Epithelial-Mesenchymal Transition, Migration, and Invasion in Triple-Negative Breast Cancer Cells," *Mol Cancer Res*, vol. 17, no. 11, pp. 2184-2195, Nov 2019, doi: 10.1158/1541-7786.MCR-18-1194.
- [19] "Statement on Sarcoidosis," *American Journal of Respiratory and Critical Care Medicine*, vol. 160, no. 2, pp. 736-755, 1999, doi: 10.1164/ajrccm.160.2.ats4-99.
- [20] G. Raghu *et al.*, "Diagnosis of Idiopathic Pulmonary Fibrosis. An Official ATS/ERS/JRS/ALAT Clinical Practice Guideline," *Am J Respir Crit Care Med*, vol. 198, no. 5, pp. e44-e68, Sep 1 2018, doi: 10.1164/rccm.201807-1255ST.
- [21] F. Van Den Hoogen *et al.*, "2013 classification criteria for systemic sclerosis: an American college of rheumatology/European league against rheumatism collaborative initiative," *Annals of the Rheumatic Diseases*, vol. 72, no. 11, pp. 1747-1755, 2013-11-01 2013, doi: 10.1136/annrheumdis-2013-204424.
- [22] N. A. Braun *et al.*, "Blockade of the Programmed Death-1 Pathway Restores Sarcoidosis CD4<sup>+</sup> T-Cell Proliferative Capacity," *American Journal of Respiratory and Critical Care Medicine*, vol. 190, no. 5, pp. 560-571, 2014-09-01 2014, doi: 10.1164/rccm.201401-0188oc.
- [23] K. A. Oswald-Richter *et al.*, "Cellular Responses to Mycobacterial Antigens Are Present in Bronchoalveolar Lavage Fluid Used in the Diagnosis of Sarcoidosis," *Infection and Immunity*, vol. 77, no. 9, pp. 3740-3748, 2009-09-01 2009, doi: 10.1128/iai.00142-09.
- [24] K. A. Oswald-Richter *et al.*, "Multiple mycobacterial antigens are targets of the adaptive immune response in pulmonary sarcoidosis," *Respiratory Research*, vol. 11, no. 1, p. 161, 2010-12-01 2010, doi: 10.1186/1465-9921-11-161.
- [25] A. A. Singh *et al.*, "Optimized ChIP-seq method facilitates transcription factor profiling in human tumors," *Life Science Alliance*, vol. 2, no. 1, p. e201800115, 2019-02-01 2019, doi: 10.26508/lsa.201800115.
- [26] H. Li and R. Durbin, "Fast and accurate short read alignment with Burrows-Wheeler transform," *Bioinformatics*, vol. 25, no. 14, pp. 1754-60, Jul 15 2009, doi: 10.1093/bioinformatics/btp324.
- [27] Y. Zhang *et al.*, "Model-based Analysis of ChIP-Seq (MACS)," *Genome Biology*, vol. 9, no. 9, p. R137, 2008-11-01 2008, doi: 10.1186/gb-2008-9-9-r137.
- [28] W. E. Lawson *et al.*, "Endoplasmic reticulum stress enhances fibrotic remodeling in the lungs," *Proc Natl Acad Sci U S A*, vol. 108, no. 26, pp. 10562-7, Jun 28 2011, doi: 10.1073/pnas.1107559108.
- [29] R.-H. Hübner *et al.*, "Standardized quantification of pulmonary fibrosis in histological samples," *BioTechniques*, vol. 44, no. 4, pp. 507-517, 2008-04-01 2008, doi: 10.2144/000112729.
- [30] S. Udalov *et al.*, "Effects of phosphodiesterase 4 inhibition on bleomycin-induced pulmonary fibrosis in mice," *BMC Pulmonary Medicine*, vol. 10, no. 1, p. 26, 2010-12-01 2010, doi: 10.1186/1471-2466-10-26.
- [31] J. D. Herazo-Maya *et al.*, "Validation of a 52-gene risk profile for outcome prediction in patients with idiopathic pulmonary fibrosis: an international, multicentre, cohort study," *The Lancet Respiratory Medicine*, vol. 5, no. 11, pp. 857-868, 2017-11-01 2017, doi: 10.1016/s2213-2600(17)30349-1.
- [32] S. L. Collins *et al.*, "Vaccinia vaccine-based immunotherapy arrests and reverses established pulmonary fibrosis," *JCI Insight*, vol. 1, no. 4, 2016-04-07 2016, doi: 10.1172/jci.insight.83116.
- [33] J. W. Card *et al.*, "Gender differences in murine airway responsiveness and lipopolysaccharide-induced inflammation," *J Immunol*, vol. 177, no. 1, pp. 621-30, Jul 1 2006, doi: 10.4049/jimmunol.177.1.621.
- [34] W. E. Lawson *et al.*, "Endoplasmic reticulum stress enhances fibrotic remodeling in the lungs," *Proceedings of the National Academy of Sciences*, vol. 108, no. 26, pp. 10562-10567, 2011-06-28 2011, doi: 10.1073/pnas.1107559108.
- [35] E. P. Consortium, "An integrated encyclopedia of DNA elements in the human genome," in *Nature* vol. 489, ed, 2012, pp. 57-74.
- [36] D. Li, S. Hsu, D. Purushotham, R. L. Sears, and T. Wang, "WashU Epigenome Browser update 2019," *Nucleic Acids Res*, vol. 47, no. W1, pp. W158-W165, Jul 2 2019, doi: 10.1093/nar/gkz348.
- [37] M. S. Caetano *et al.*, "Sex specific function of epithelial STAT3 signaling in pathogenesis of K-ras mutant lung cancer," *Nat Commun*, vol. 9, no. 1, p. 4589, Nov 2 2018, doi: 10.1038/s41467-018-07042-y.

- [38] J. F. Couse and K. S. Korach, "Estrogen Receptor Null Mice: What Have We Learned and Where Will They Lead Us?," *Endocrine Reviews*, vol. 20, no. 3, pp. 358-417, 1999-06-01 1999, doi: 10.1210/edrv.20.3.0370.
- [39] O. S. Chioma *et al.*, "Gut microbiota modulates lung fibrosis severity following acute lung injury in mice," *Commun Biol*, vol. 5, no. 1, p. 1401, Dec 22 2022, doi: 10.1038/s42003-022-04357-x.
- [40] D. N. O'Dwyer *et al.*, "Lung Microbiota Contribute to Pulmonary Inflammation and Disease Progression in Pulmonary Fibrosis," *Am J Respir Crit Care Med*, vol. 199, no. 9, pp. 1127-1138, May 1 2019, doi: 10.1164/rccm.201809-1650OC.
- [41] A. M. Tyagi *et al.*, "The Microbial Metabolite Butyrate Stimulates Bone Formation via T Regulatory Cell-Mediated Regulation of WNT10B Expression," *Immunity*, vol. 49, no. 6, pp. 1116-1131 e7, Dec 18 2018, doi: 10.1016/j.jimmuni.2018.10.013.
- [42] M. D. Mora-Ruiz, F. Blanco-Favela, A. K. Chavez Rueda, M. V. Legorreta-Haquet, and L. Chavez-Sanchez, "Role of interleukin-17 in acute myocardial infarction," *Mol Immunol*, vol. 107, pp. 71-78, Mar 2019, doi: 10.1016/j.molimm.2019.01.008.
- [43] J. Pfeilschifter, S. M. Seyedin, and G. R. Mundy, "Transforming growth factor beta inhibits bone resorption in fetal rat long bone cultures," *Journal of Clinical Investigation*, vol. 82, pp. 680-685, 1988, doi: 10.1172/jci113647.
- [44] S. Elliot *et al.*, "MicroRNA let-7 Downregulates Ligand-Independent Estrogen Receptor-mediated Male-Predominant Pulmonary Fibrosis," *Am J Respir Crit Care Med*, vol. 200, no. 10, pp. 1246-1257, Nov 15 2019, doi: 10.1164/rccm.201903-0508OC.
- [45] G. N. Huang, J. Xu, D. E. Lefever, T. C. Glenn, T. Nagy, and T. L. Guo, "Genistein prevention of hyperglycemia and improvement of glucose tolerance in adult non-obese diabetic mice are associated with alterations of gut microbiome and immune homeostasis," (in English), *Toxicol Appl Pharm*, vol. 332, pp. 138-148, Oct 1 2017, doi: 10.1016/j.taap.2017.04.009.
- [46] R. Flores *et al.*, "Fecal microbial determinants of fecal and systemic estrogens and estrogen metabolites: a cross-sectional study," (in English), *J Transl Med*, vol. 10, Dec 21 2012, doi: Artn 253  
10.1186/1479-5876-10-253.
- [47] S. M. Ervin *et al.*, "Gut microbial  $\beta$ -glucuronidases reactivate estrogens as components of the estrobolome that reactivate estrogens," (in eng), *J Biol Chem*, vol. 294, no. 49, pp. 18586-18599, Dec 6 2019, doi: 10.1074/jbc.RA119.010950.
- [48] Y. Sui, J. M. Wu, and J. P. Chen, "The Role of Gut Microbial beta-Glucuronidase in Estrogen Reactivation and Breast Cancer," (in English), *Front Cell Dev Biol*, vol. 9, Aug 12 2021, doi: ARTN 631552  
10.3389/fcell.2021.631552.
- [49] D. C. Newcomb *et al.*, "Estrogen and progesterone decrease let-7f microRNA expression and increase IL-23/IL-23 receptor signaling and IL-17A production in patients with severe asthma," *Journal of Allergy and Clinical Immunology*, vol. 136, no. 4, pp. 1025-1034.e11, 2015, doi: 10.1016/j.jaci.2015.05.046.
- [50] H. Fuseini *et al.*, "ERalpha Signaling Increased IL-17A Production in Th17 Cells by Upregulating IL-23R Expression, Mitochondrial Respiration, and Proliferation," *Front Immunol*, vol. 10, p. 2740, 2019, doi: 10.3389/fimmu.2019.02740.
- [51] L. Dong, C. Qin, Y. Li, Z. Wu, and L. Liu, "Oat phenolic compounds regulate metabolic syndrome in high fat diet-fed mice via gut microbiota," *Food Bioscience*, vol. 50, 2022, doi: 10.1016/j.fbio.2022.101946.
- [52] Y. Li *et al.*, "Whole grain benefit: synergistic effect of oat phenolic compounds and beta-glucan on hyperlipidemia via gut microbiota in high-fat-diet mice," *Food & Function*, vol. 13, no. 24, pp. 12686-12696, Dec 13 2022, doi: 10.1039/d2fo01746f.
- [53] L. Liu *et al.*, "Consumption of the Fish Oil High-Fat Diet Uncouples Obesity and Mammary Tumor Growth through Induction of Reactive Oxygen Species in Protumor Macrophages," *Cancer Research*, vol. 80, no. 12, pp. 2564-2574, Jun 15 2020, doi: 10.1158/0008-5472.CAN-19-3184.